Purification of molybdenum, growth and characterization of medium volume $ZnMoO_4$ crystals for the LUMINEU program

2014 JINST 9 P06004

(http://iopscience.iop.org/1748-0221/9/06/P06004)

PUBLISHED BY IOP PUBLISHING FOR SISSA MEDIALAB
RECEIVED: *February 23, 2014*
REVISED: *April 1, 2014*
ACCEPTED: *April 14, 2014*
PUBLISHED: *June 4, 2014*

Purification of molybdenum, growth and characterization of medium volume $ZnMoO_4$ crystals for the LUMINEU program

L. Bergé,[a] R.S. Boiko,[b] M. Chapellier,[a] D.M. Chernyak,[a,b] N. Coron,[c] F.A. Danevich,[b] R. Decourt,[d] V.Ya. Degoda,[e] L. Devoyon,[f] A. Drillien,[a] L. Dumoulin,[a] C. Enss,[g] A. Fleischmann,[g] L. Gastaldo,[g] A. Giuliani,[a,i,j,1] M. Gros,[f] S. Herve,[f] V. Humbert,[a] I.M. Ivanov,[h] V.V. Kobychev,[b] Ya.P. Kogut,[e] F. Koskas,[f] M. Loidl,[f] P. Magnier,[f] E.P. Makarov,[h] M. Mancuso,[a,i] P. de Marcillac,[c] S. Marnieros,[a] C. Marrache-Kikuchi,[a] S.G. Nasonov,[h] X.F. Navick,[f] C. Nones,[f] E. Olivieri,[a] B. Paul,[f] Y. Penichot,[f] G. Pessina,[j] O. Plantevin,[a] D.V. Poda,[a,b] T. Redon,[c] M. Rodrigues,[f] V.N. Shlegel,[h] O. Strazzer,[f] M. Tenconi,[a] L. Torres,[c] V.I. Tretyak,[b] Ya.V. Vasiliev,[h] M. Velazquez,[d] O. Viraphong[d] and V.N. Zhdankov[k]

[a] *Centre de Sciences Nucléaires et de Sciences de la Matière, Bâtiment 104/108, Campus d'Orsay, 91405 Orsay, France*
[b] *Institute for Nuclear Research, b47 prospekt Nauky, MSP 03680 Kyiv, Ukraine*
[c] *IAS, UMR 8617 Université Paris-Sud 11/CNRS, Bâtiment 121, 91405 Orsay, France*
[d] *CNRS, Université de Bordeaux, ICMCB, 87 avenue du Dr. A. Schweitzer, 33608 Pessac cedex, France*
[e] *Kyiv National Taras Shevchenko University, 64 Volodymyrs'ka Str., 01601 Kyiv, Ukraine*
[f] *CEA-Saclay, F-91191 Gif sur Yvette, France*
[g] *Institut für Angewandte Physik, Universität Heidelberg, Albert-Ueberle-Strasse 3-5, D-69120 Heidelberg, Germany*
[h] *Nikolaev Institute of Inorganic Chemistry, 3 Acad. Lavrentieva Ave., 630090 Novosibirsk, Russia*
[i] *Dipartimento di Scienza e Alta Tecnologia, Università dell'Insubria, Via Valleggio 11, 22100 Como, Italy*
[j] *Dipartimento di Fisica dell'Università e Sezione di Milano-Bicocca dell'INFN, Piazza della Scienza 3, 20126 Milano, Italy*
[k] *Crystal Manifacturing Lab Ltd., 3 Acad. Lavrentieva Ave., 630090 Novosibirsk, Russia*

E-mail: Andrea.Giuliani@csnsm.in2p3.fr

[1] Corresponding author.

doi:10.1088/1748-0221/9/06/P06004

2014 JINST 9 P06004

ABSTRACT: The LUMINEU program aims at performing a pilot experiment on neutrinoless double beta decay of ^{100}Mo using radiopure $ZnMoO_4$ crystals operated as cryogenic scintillating bolometers. Growth of high quality radiopure crystals is a complex task, since there are no commercial molybdenum compounds available with the required level of purity and radioactive contamination. This paper discusses approaches to purify molybdenum and synthesize compounds for high quality radiopure $ZnMoO_4$ crystal growth. A combination of a double sublimation (with addition of zinc molybdate) with subsequent recrystallization in aqueous solutions (using zinc molybdate as a collector) was used. Zinc molybdate crystals up to 1.5 kg were grown by the low-thermal-gradient Czochralski technique; their optical, luminescent, diamagnetic, thermal and bolometric properties were tested.

KEYWORDS: Scintillators, scintillation and light emission processes (solid, gas and liquid scintillators); Hybrid detectors; Photoemission; Cryogenic detectors

2014 JINST 9 P06004

Contents

2014 JINST 9 P06004

1 Introduction

Neutrinoless double beta ($0\nu2\beta$) decay is a hypothetical rare nuclear process in which two neutrons transform into two protons emitting two beta electrons and nothing else. This transition is forbidden in the standard model (SM) since it violates the lepton number by two units, but it is expected in those extensions of the SM which describe the neutrino as a massive Majorana fermion, i.e. equal to its own antiparticle. Therefore, the search for the $0\nu2\beta$ decay is considered as a method — the only one experimentally viable — to test the Majorana nature of neutrino and lepton number conservation. The $0\nu2\beta$ decay may be induced by the exchange of a virtual light Majorana neutrino (the so-called mass mechanism), right-handed currents in the weak interactions and many other effects beyond the SM (see ref. [1–4] and references therein). Recent neutrino oscillation experiments indicate that neutrinos are massive. However, the oscillation experiments are sensitive to the differences between squared neutrino masses, while the absolute neutrino mass scale remains unknown [5–7]. Neutrinoless double beta decay, if mediated by the mass mechanism, is able not only to ascertain the Majorana nature of neutrino but also to measure the effective Majorana neutrino mass $\langle m_\nu \rangle$, related to the absolute neutrino mass scale, and, in some regions of the neutrino mass parameter space, to determine the hierarchy of neutrino masses.

While the two neutrino double beta decay — allowed in the SM — has been detected in 11 isotopes with half-lives in the range $T_{1/2} \sim 10^{18}$–10^{24} yr [8, 9], the $0\nu2\beta$ decay remains unobserved at a sensitivity level up to $T_{1/2} \sim 10^{23}$–10^{25} yr [10]. A near goal of the projected $0\nu2\beta$ experiments is to test the inverted neutrino mass hierarchy scenario (corresponding to an effective Majorana

Table 1. Properties of $ZnMoO_4$ crystal scintillators.

Property	Value	Reference
Density (g/cm^3)	4.3	[25]
Melting point (°C)	1003 ± 5	[26]
Structural type	Triclinic, $P1$	[25, 26]
Cleavage plane	Weak (001)	[25]
Hardness on the Mohs scale	3.5	[24]
Index of refraction (in the wavelength interval 406–532 nm)	1.87–2.01	[24]
Wavelength of emission maximum (nm)	585–625	[24, 25, 27]
Light yield (photon/MeV) at 10 K	5×10^3	[28]
Quenching factor for α particles of ~ 5 MeV	0.15–0.19	[23, 24], This work
Debye temperature (K)	625	This work

neutrino mass in the range 0.02–0.05 eV), which demands an experimental sensitivity at the level of $T_{1/2} \sim 10^{26} - 10^{27}$ years [3].

Searching for so rare decays requires large detectors, containing hundreds of kg of the isotope of interest, with high energy resolution and detection efficiency, and as low as possible (ideally zero) background. The choice of the nucleus to be studied is a crucial element too. The isotope ^{100}Mo is one of the most promising candidates to search for $0\nu2\beta$ decay thanks to the high energy of the process ($Q_{2\beta} = 3034.40(17)$ keV [11]), a reasonable natural isotopic abundance ($\delta = 9.824(50)\%$ [12]), and favourable theoretical predictions (see ref. [3] and references therein). The most stringent half-life limit on the $0\nu2\beta$ decay of ^{100}Mo was set in the NEMO3 experiment at the level of $T_{1/2} \geqslant 10^{24}$ years at 90% confidence level [13].

Low temperature scintillating bolometers satisfy the aforementioned requirements. This technique looks extremely promising to search for $0\nu2\beta$ decay in ^{82}Se, ^{100}Mo and ^{116}Cd thanks to high energy resolution (a few keV) and detection efficiency (70–90%, depending on crystal scintillator composition and size), and the possibility to reach a very low background counting rate (a few counts / (yr $\times$ keV $\times$ ton)) in the region of interest [14–20].

The LUMINEU (Luminescent Underground Molybdenum Investigation for NEUtrino mass and nature) project is based on a recently developed technique to grow large high quality radiopure zinc molybdate ($ZnMoO_4$) crystal scintillators [18, 19, 21–24], which makes this material advantageous for low temperature bolometric experiments to search for $0\nu2\beta$ decay of ^{100}Mo. The project aims to set the bases for a next-generation $0\nu2\beta$ decay experiment capable to explore the inverted hierarchy region of the neutrino mass pattern with the help of a large array of scintillating bolometers based on $ZnMoO_4$ crystals containing the isotope ^{100}Mo. The expected sensitivity of the final stage of the LUMINEU programme (assuming a low-background underground array of about 40 $ZnMO_4$ scintillators with a size of $\varnothing 60 \times 40$ mm and containing 10 kg of enriched ^{100}Mo) is similar to the current major double-beta decay experiments and already approaches the onset of the inverted hierarchy region [18]. Extensions of this search up to the 100–1000 kg scale would enable a full test of the inverted hierarchy region. The properties of $ZnMoO_4$ crystal scintillators are presented in table 1.

2014 JINST 9 P06004

Radioactive contamination of $ZnMoO_4$ crystal scintillators is one of the most important issues to be addressed in the material R&D. High purity molybdenum and zinc are required to grow high quality radiopure $ZnMoO_4$ crystal scintillators. While a high purity zinc oxide is commercially available, molybdenum should be additionally purified. Contamination of the crystal scintillators with ^{228}Th and ^{226}Ra is particularly harmful: activities of these nuclides should not exceed the level of 0.01 mBq/kg [18]. A total alpha activity of the U/Th daughters (mainly ^{210}Po, daughter of ^{210}Pb from the ^{238}U chain, for which secular equilibrium is typically broken) and activity of ^{40}K are requested to be very low as well (approximately down to the mBq/kg level), because of the rather slow response of cryogenic bolometers. It is to remark that so low activities correspond to rather low concentrations of thorium, uranium and potassium at the level of $\sim$ ppt (for thorium), ~ 0.1 ppb (uranium) and ~ 0.1 ppm (potassium). These concentrationss are hard to measure even by the most sensitive analytical methods, like mass-spectrometry. At the same time, there are no commercial molybdenum compounds available with the required level of purity and radioactive contamination. Tests of the raw materials for crystal growth are therefore extremely difficult and require long measurements. Activities so low of ^{228}Th and ^{226}Ra are not measurable even by the most sensitive low-background HPGe gamma detectors [29]. Typically, high sensitivity radiopurity tests can be done only after crystal growth using calorimetric methods. Optical and scintillation quality of the scintillators depends on trace impurities at the 0.1 ppm–10 ppm level. Moreover, the development of efficient purification methods with minimal losses of molybdenum is strongly required to produce $ZnMoO_4$ crystals from enriched molybdenum, for which the impurity concentration is typically at the level of tens–hundreds ppm and radioactive contamination (2 mBq/kg of ^{226}Ra, 0.6 mBq/kg of ^{228}Th and 36 mBq/kg of ^{40}K [30]) substantially exceeds the acceptable level.

The main goals of the purification/crystallization processes are to achieve: a) a low enough level of radioactive contamination of $ZnMoO_4$ crystal scintillators; b) high scintillation and optical quality of the material; c) stable and reproducible growing procedure to obtain a maximal output of scintillation elements with required shape and size; d) minimal losses of molybdenum (taking into account the future plans to produce scintillators from the expensive enriched isotope and the necessity to recycle the costly enriched material). It should be stressed that the progress in $ZnMoO_4$ crystal growth was achieved mainly thanks to additional purification of molybdenum [24].

Here we report further progresses in deep purification of molybdenum and growth of $ZnMoO_4$ crystals for the LUMINEU project. First results of the crystals characterization are presented too.

2 Production of $ZnMoO_4$ crystals

2.1 Purification of molybdenum

We have developed a two-stage technique of molybdenum purification consisting of sublimation of molybdenum oxide in vacuum (with addition of zinc molybdate) and double recrystallization from aqueous solutions by co-precipitation of impurities on zinc molybdate sediment. Samples of molybdenum with natural isotopic composition were used in the present work.

2.1.1 Purification of MoO_3 by sublimation

Sublimation of molybdenum oxide under atmospheric pressure with subsequent leaching in aqueous solutions with ammonia is widely used in the industry of molybdenum. However, the concen-

2014 JINST 9 P06004

tration of impurities, particularly of tungsten (at the level of up to 0.5wt% even in the high purity grade materials) still exceeds the $ZnMoO_4$ crystal growth requirements. Even additional vacuum sublimation of molybdenum oxide proved to be insufficient. According to ref. [31] separation of tungsten and molybdenum is a well-known problem. Besides, the sublimation of MoO_3 is not efficient enough to reduce traces e.g. of Ca, Na and Si to the level below 20–70 ppm.

We have assumed that during sublimation at high temperature the following exchange reaction could occur:

$$ZnMoO_4 + WO_3 = ZnWO_4 + MoO_3 \uparrow . \tag{2.1}$$

Such a reaction should reduce the concentration of tungsten, and therefore can be used for separation of molybdenum from tungsten. To prove this possibility, we have prepared a sample of MoO_3 powder with 10wt% of WO_3. The concentration of tungsten in the MoO_3 product after sublimation was reduced to 0.1wt%.

One more confirmation of the method's efficiency was obtained by chemical and X-ray diffraction analysis of the rests after the sublimations performed with the aim to purify molybdenum for crystal growth (the amount of the rests is typically 1–3 wt% of the initial amount of the purified material). The bottoms after a few sublimation processes were mixed and annealed in air atmosphere to oxidize residues of metals. Then we have carried out sublimation of the sample in vacuum to reduce presence of MoO_3. Atomic emission analysis, performed in the analytical laboratory of the Nikolaev Institute of Inorganic Chemistry, gives the following elemental composition of the bottoms: Ca — 0.14wt%; Cu — 0.011wt%; Fe — 0.064wt%; K — 1wt%; Mg — 0.026wt%; Na — 0.13wt%; Si — 2.6wt%; Mo — 22wt%; W — 18wt%; Zn — 14wt%. Oxides of molybdenum and silicon, tungstate (in form of tungstate-molybdate) and molybdate of zinc, as well as $K_2Mo_7O_{22}$ and $K_2MgSi_5O_{12}$, have been identified in the bottoms with the help of X-ray diffraction analysis. At the same time, tungsten oxide (present in the initial product) was not detected in the bottoms. The data supported occurring of the exchange reaction (2.1) and confirmed efficiency of molybdenum oxide sublimation in vacuum with addition of zinc molybdate.

In order to purify molybdenum for $ZnMoO_4$ crystal growth, we have added up to 1% of high purity zinc molybdate (obtained earlier in the course of the R&D) to the MoO_3 prepared for sublimation. The obtained sublimates contained a mixture of molybdenum oxides of different composition and color, which hinders their use for $ZnMoO_4$ synthesis. The sublimates were then annealed in air atmosphere to obtain yellow color stoichiometric MoO_3. The sublimates were analyzed by atomic emission spectrometry. The results are presented in table 2. One can see that the purity level of MoO_3 was improved by one-two orders of magnitude after the double sublimation process. The sublimation also should remove metal oxides, which have a high vapor pressure at temperatures up to a thousand degrees.

2.1.2 Purification by recrystallization from aqueous solutions

Finally the molybdenum was purified by double recrystallization of ammonium molybdate in aqueous solutions with the deposition of impurities on zinc molybdate sediment. For this purpose molybdenum oxide was dissolved in solution of ammonia at room temperature. Mono-molybdates and various poly-compounds and hetero-poly compounds are formed depending on the mixing ratio of the components. The composition of the compounds depends on the acidity of the solution

2014 JINST 9 P06004

Table 2. Efficiency of molybdenum oxide purification by sublimation.

Material	Concentration of impurities (ppm)			
	Si	K	Fe	W
Initial MoO_3	600	100–500	6	200–500
After 1st sublimation	100–500	10–50	2–6	100–200
After 2nd sublimation	70	1–8	< 1	30–40

and components concentration. Molybdates in aqueous solutions form normal molybdate:

$$MoO_3 + 2NH_4OH = (NH_4)_2MoO_4 + H_2O \tag{2.2}$$

and ammonium hepta-molybdates, $(NH_4)_xH_{(6-x)}[Mo_7O_{24}]$. Poly-molybdates can form, in presence of impurities, during long time exposure, ammonium salts of silico-molybdic and phosphor-molybdic acids, for instance $H_8[Si(Mo_2O_7)_6]$, $H_7[P(Mo_2O_7)_6]$. Apart from Si(IV) and P(V), also V(V), Ge(IV), Cr(III), etc. can play the role of the central atom, while ligands of the inner sphere can be ions WO_4^{2-}, VO^{3-}, CrO_4^{2-}, TeO_4^{2-}. Solutions of poly-molybdates at pH < 6 are able to dissolve oxides and hydroxides of many metals, e.g. ZnO, $Fe(OH)_3$, $Ni(OH)_2$, $Cu(OH)_2$, etc. As a result, a partial co-crystallization of impurities could occur. Thus, recrystallization of ammonium para-molybdate is not efficient enough for molybdenum purification. Besides, a typical concentration of impurities in high purity commercial MoO_3 is relatively low (1–100 ppm). As a result, the impurity sediments appear in a form of fine microcrystals, hardly removable by filtration.

To improve efficiency of the recrystallization process, we have used zinc oxide to initiate precipitation (taking into account that zinc does not affect the crystal quality). ZnO at the level of 1–2 g/L was dissolved in the ammonium para-molybdate solution at pH > 6, then ammonia was added to the solution to reach pH = 7–8. After several hours of exposure precipitation of zinc molybdate occurs. The $ZnMoO_4$ sediment sorbs impurities from the solution. Further increasing of pH leads to precipitation of contaminants in the form of hydroxides. It should be stressed, that the basic solution with pH $\approx$ 8–9 provides the most favorable conditions for thorium and uranium precipitation. After separation of the sediment, the solution was evaporated to 70% at temperature near the boiling point of the solution. Then ammonium oxalate was added to the solution to bind the residues of iron impurities. Results of the purification are presented in table 3.

It should be also stressed that using of the additional "wet" chemistry procedure is also encouraged by the fact that large crystal grains of MoO_3 are formed in the sublimation process, which adds certain difficulties to produce radiopure $ZnMoO_4$ powder (an additional procedure of the oxide grains grinding could contaminate the material). Subsequent dissolution of the molybdenum oxide in ammonia allows to obtain high purity MoO_3 perfectly fine for further synthesis of $ZnMoO_4$ powder.

The molybdenum oxide purified by double recrystallization procedure from aqueous solutions and high purity grade zinc oxide (ZnO) produced by the company UMICORE were used to synthesize $ZnMoO_4$ powder for crystal growth.

2014 JINST 9 P06004

2.2 $ZnMoO_4$ crystal growth

Several $ZnMoO_4$ crystal boules were grown in air atmosphere from the purified input powder by the low-thermal-gradient Czochralski technique [32–34] in platinum crucibles ∅40 and ∅80 mm (it should be mentioned that, according to the certificates of the platinum crucibles, iron content in the platinum does not exceed 40 ppm). The temperature gradient was kept below 1 K/cm, the rotational speed was in the range of 5–20 rotations per minute with the crystallization rate of 0.8–1.2 mm/hour. A low crystallization rate was kept during growing of the upper cone of the crystal boules. Rotational speed was decreased from the start to the end of the growth process by 1.5–2 times. The yield of the produced boules was at the level of 80%, which is an important achievement taking into account the future plans to produce crystals from enriched ^{100}Mo. Four optical elements (two ∅20 × 40 mm and two ∅35 × 40 mm with masses 55 g and 160 g, respectively) were cut and polished for low temperature measurements. Several small samples were produced for optical, luminescent, diamagnetic and thermal tests.

Contamination of a sample of the produced $ZnMoO_4$ crystals was measured by using Glow discharge mass spectrometry. The results of the analysis are presented in table 3.

3 Characterization of $ZnMoO_4$ crystals

3.1 Optical absorption

Visible and near infrared absorption spectra of $ZnMoO_4$ crystal were recorded with a Varian Cary 5000 spectrophotometer. The transmission coefficient, T, was measured on a 2.0 mm-thick single crystal and found to be higher than 0.5 from 327 nm to 4.96 μm. The absorption coefficient was calculated as $\alpha = -\log T \times \ln 10/t$, with t the thickness of the crystal. The data are presented in figure 1.

The cut-off wavelengths are 313 nm (≈ 3.96 eV) and 5.13 μm. The absorption coefficient decreases from 1.47 to 0.89 cm^{-1} in the wavelength region from 400 nm to 2 μm, but there does not seem to be a broad absorption band around 440 nm that could be ascribed to Fe^{2+}/Fe^{3+} impurities as described in [28] and [35]. This is due to the low Fe concentration in the crystal ($\approx 1.71 \times 10^{16}$ cm^{-3}) and in fact, it can be stated that a safe detection limit around 440 nm by such transmission experiments is $\sim 10^{18}$ atoms of Fe per cm^3. Such a low absorption coefficient turns out to be lower than that of the orange crystals grown in [25] and [36], which exhibit $\alpha_{abs}(< 550\,\text{nm}) \geqslant 2.5\,\text{cm}^{-1}$. The refractive index at 650 nm, obtained from $1 + (1 - T^2)^{1/2}/T$ (no Fresnel losses), is ≈ 1.96, close to the value ∼ 1.91 given in [37] and to the values 1.87–2.01 (taking into account biaxiality of the material) obtained in [24] for the wavelengths 406–655 nm.

Finally, taking n(589 nm) = 1.91 (determined with a Na lamp [37]), solving self-consistently $R = (1 + \exp(-\alpha \times t)) \times ((n-1)/(n+1))^2$ and $\alpha = -\log(T + R) \times (\ln 10)/t$, one obtains $\alpha(589\,\text{nm}) = 0.023\,\text{cm}^{-1}$, which leads to an attenuation length of 43 cm at this wavelength. It should be stressed the transmittance of the produced crystal even exceeds the requirements of the LUMINEU project (attenuation length more than 30 cm at the emission maximum ≈ 600 nm [24]).

2014 JINST 9 P06004

Table 3. Purity level of MoO_3 before and after purification by recrystallization and sublimation. Data for commercial 5N5 grade product and enriched ^{100}Mo material are given for comparison.

Material	Concentration of impurities (ppm)							
	Na	Mg	Si	K	Ca	Fe	Zn	W
Initial MoO_3	60	1	60	50	60	8	10	200
Recrystallization from aqueous solutions	30	< 1	30	20	40	6	1000	220
Sublimation and recrystallization from aqueous solutions	–	< 1	30	10	12	5	500	130
Double sublimation and recrystallization from aqueous solutions	–	< 1	–	< 10	< 10	< 5	70	< 50
5N5 grade MoO_3 used to produce $ZnMoO_4$ crystal studied in [21, 27]	24	–	9	67	15	< 18	–	96
Samples of enriched isotope ^{100}Mo used in [30] (before purification, data of producer)	10	< 10	50–360	< 30	40–50	10–80	–	200
$ZnMoO_4$ crystal	0.36	0.72	0.09	0.14	0.13	0.38	–	190

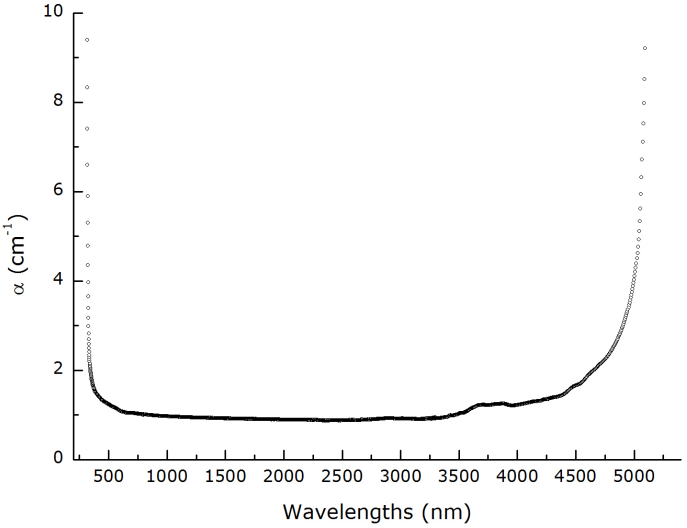

Figure 1. Absorption of 2 mm thick $ZnMoO_4$ single crystal. α denotes absorption coefficient.

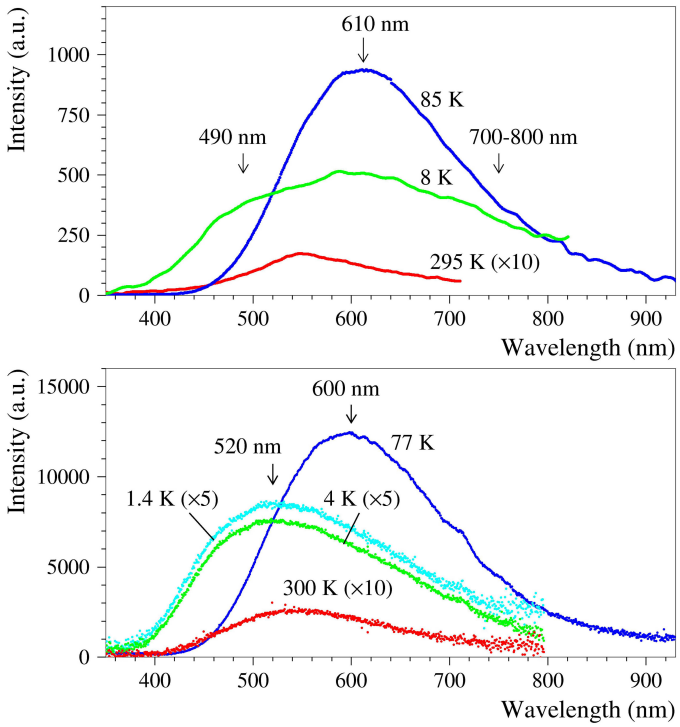

Figure 2. Emission spectra of $ZnMoO_4$ crystal under X-ray excitation at different temperatures measured in Kyiv (upper part) and Orsay (lower part).

3.2 Luminescence under X-ray excitation

The luminescence of the $ZnMoO_4$ crystal sample ($10 \times 10 \times 2$ mm) was investigated as a function of temperature between 8 and 290 K under X-ray excitation at the Department of Physics of the Kyiv National Taras Shevchenko University. The sample was irradiated by X-rays from a BHV7 tube with a rhenium anode (20 kV, 20 mA). Light from the crystal was detected in the visible region by a FEU-106 photomultiplier (sensitive in the wide wavelength region of 350–820 nm) and in the near infrared region by a FEU-83 photomultiplier (with enhanced sensitivity up to $\approx 1\,\mu$m). Spectral measurements were carried out using a high-aperture MDR-2 monochromator. Emission spectra measured at 8 K, 85 K and 295 K, corrected for the spectral sensitivity of the registration system, are shown in figure 2 (upper part). There are at least three emission bands in the spectra with maxima at 490 nm, 610 nm and a near infrared emission at 700–800 nm. The most intensive luminescence with a maximum at ≈ 610 nm was observed at liquid nitrogen temperature.

The observation was confirmed in similar measurements performed at the Institut d'Astrophysique Spatiale in Orsay. A $ZnMoO_4$ sample $\varnothing 20 \times 6$ mm was irradiated through a beryllium window and an aluminium thin foil using an X-ray micro-tube (Bullet type from Moxtek; HV = 40 kV; I = 100 uA). The sample was cooled in a reflecting cavity in a home made cryostat and the light was transmitted by an optical fiber outside, up to an AVANTES 2048 spectrometer. The emission spectra (see lower part of figure 2) were accumulated over 20 s, the data were taken after long enough stabilization of the light emission level after switching the tube off. Being qualitatively similar to the data obtained in Kyiv, the shape of the spectra and the relative intensities of the bands are slightly different. The difference can be explained by using of different samples and doses.

2014 JINST 9 P06004

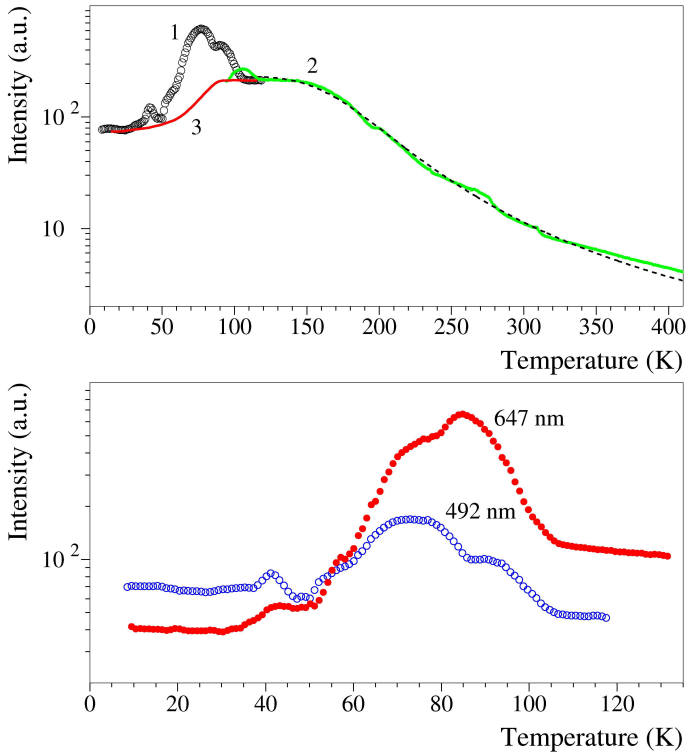

Figure 3. (Upper part) Dependence of $ZnMoO_4$ luminescence intensity under X-ray excitation in a wide interval of emission spectrum on temperature measured in the temperature interval 8–120 K (1) and 85–410 K (2). Curve 3 represents dependence of luminescence intensity on temperature after subtraction of thermally stimulated luminescence (see text and figure 4). (Lower part) Temperature dependence of short wavelength (492 nm) and long wavelength (647 nm) luminescence.

Dependence of $ZnMoO_4$ luminescence intensity on temperature measured in Kyiv (see figure 3) is again in agreement with the previous results [24]. The temperature dependence of luminescence above 120 K can be described by the Mott formula:

$$\frac{J(T)}{J_0} = \frac{1}{1 + A \cdot \exp\left(-\frac{E_T}{kT}\right)} \tag{3.1}$$

where $J(T)$ is luminescence intensity at temperature T, J_0 is luminescence intensity at temperature $T \rightarrow 0$, k is the Boltzmann constant. A fit of the temperature dependence in the interval 120–410 K (see dashed line on upper part of figure 3) gives rather low value of the damping energy $E_T = 0.12$ eV. It should be stressed that we have observed a clear difference in the temperature behaviour of the short (492 nm) and long wavelength (647 nm) emission (see lower part of figure 3), which confirms further our assumption about different nature of the emission bands.

Thermo-stimulated luminescence (TSL) of $ZnMoO_4$ was studied after X-ray excitation during 20 min at 8 K and at 85 K (see figure 4). We have observed a very intensive TSL at 78 K after irradiation at 8 K. There is a clear TSL peak at 114 K and several smaller peaks at higher temperature after irradiation of the sample at 85 K. The observed intense TSL with numerous peaks in a wide temperature interval indicates the presence of point defects in the sample.

2014 JINST 9 P06004

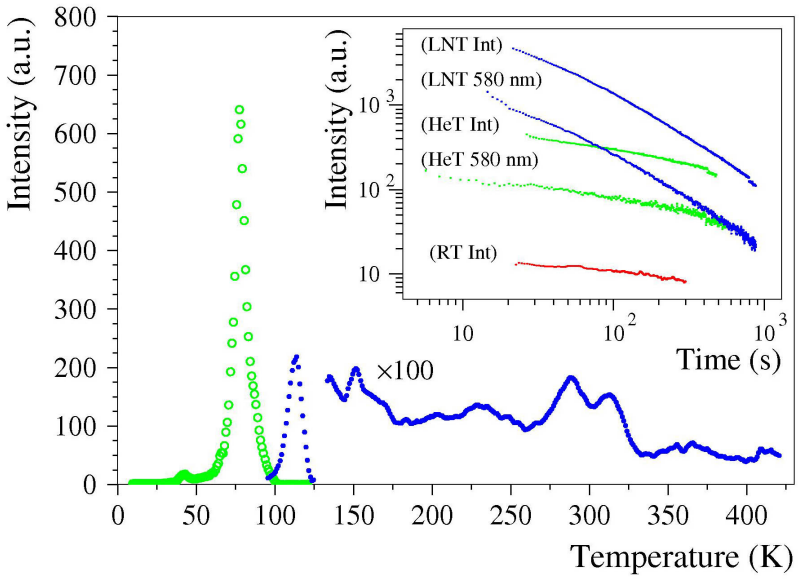

Figure 4. Thermally stimulated luminescence of $ZnMoO_4$ crystal after X-ray excitation during 20 min at 8 K (open circles) and at 85 K (filled circles). (Inset) Phosphorescence after X-ray irradiation during 20 min at 8 K (HeT), 85 K (LNT) and at room temperature 295 K (RT) in a wide interval of emission spectrum (Int) and at 580 nm.

A rather slow phosphorescence observed after the irradiation of the sample at the temperature of 8 K, 85 K and 295 K (see inset in figure 4) also confirms the presence of shallow traps due to imperfections and defects in the crystal. Besides, the difference in the phosphorescence decay time confirms a different origin of the optical bands. The traps cause the low scintillation efficiency of the sample. Further improvement of the crystal quality is still required to improve scintillation properties of the material. We hope that application of the purification methods developed in this work could answer on the question whether the crystal quality depends on the initial molybdenum pollution, particularly by tungsten traces, which contamination should be substantially reduced by application of the sublimation technique.

It should be noted that TSL and long time phosphorescence were recorded also between 1.4 K and 300 K by using the set-up in Orsay, with one intense TSL emission peak clearly detected around 50 K.

The results of our studies of $ZnMoO_4$ luminescence are in agreement with the data of previous studies [24, 25, 27, 28]. Investigation of $ZnMoO_4$ crystals luminescence is in progress. In particular we are going to study whether the luminescence is still influenced mainly by the remaining impurities or rather by structural defects of the crystal samples. The results of this research will be presented in a dedicated paper in preparation.

3.3 Magnetic susceptibility

Magnetic susceptibility was measured using a Quantum Design SQUID MPMS XL magnetometer operating in the 4.2–350 K temperature range and in the 0–5 T magnetic field range. The crystal mass was 210 mg and its volumic mass assumed to be 4.19 g/cm^3. It was mounted in a capsule

2014 JINST 9 P06004

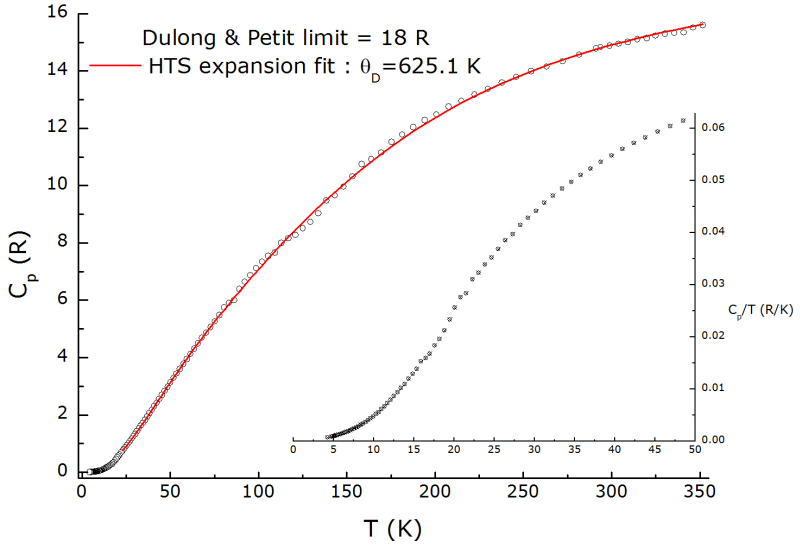

Figure 5. Specific heat *versus* temperature of a $ZnMoO_4$ single crystal. The inset shows C_p/T *vs* T at low temperature to evidence the absence of any long range order effect down to 4 K.

placed in a straw and the negligibly small diamagnetic contribution $\left(|\chi| < 10^{-7}\right)$ of the capsule was not subtracted from our data. The $ZnMoO_4$ proved to be weakly diamagnetic with a MKSA $\chi = -(8.0 \pm 0.2) \times 10^{-6}$ over the whole temperature range investigated, from 20 to 320 K. Thus, paramagnetic impurities such as Fe^{2+} or Fe^{3+} could not be evidenced even under higher applied magnetic fields up to 0.2 T.

3.4 Specific heat measurements

Specific heat measurements were made on a $3 \times 3 \times 2\,mm^3$ single crystal to optimize the exchange surface and avoid too much thermal inertia. The crystal was fixed on a sapphire sample holder with vacuum grease. The sample holder was mounted on the measurement shaft of a Quantum Design PPMS equipment interfaced to operate with a 2-τ pulse-step method corrected for the grease baseline. The results of the measurements are presented in figure 5. The phononic contribution could be approximated for temperatures higher than ~ 23 K by means of high-temperature series (HTS) expansion:

$$C_{p,ph.} \propto 1 + \sum_{i=1}^{4} B_i \left[1 + \left(2\pi \frac{T}{\theta_D}\right)^2\right]^{-i} \tag{3.2}$$

(formula (5) from [38], and red curve in figure 5), which yielded a high Debye temperature of ≈ 625 K and the following Bernoulli numbers: $B_1 = 1.9091$, $B_2 = 1.86714$, $B_3 = -0.96009$, $B_4 = -0.00907$. No long range order (LRO) effect was observed down to 4 K. The $C_p/3NR$ ratio at 351 K reaches 0.87 and remains lower than the Dulong and Petit limit, which suggests low anharmonic effects at play at this temperature, consistent with the high Debye temperature obtained by the HTS fit.

2014 JINST 9 P06004

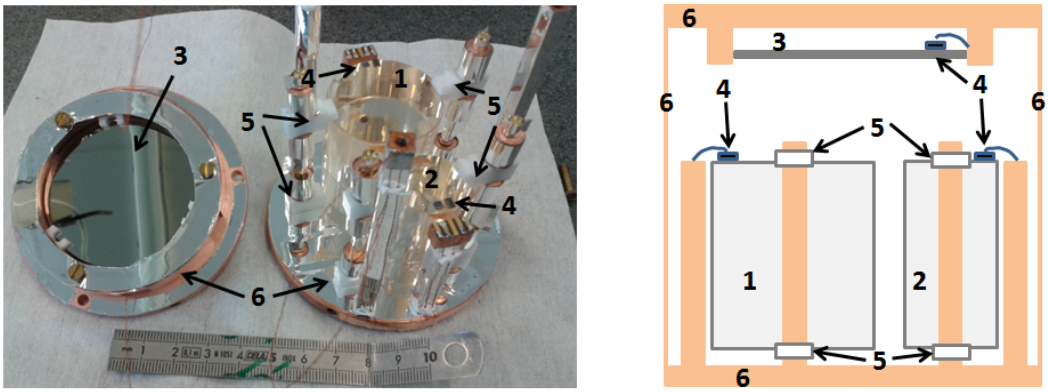

Figure 6. Photograph (right panel) and scheme (left panel) of the detectors setup: (1) $ZnMoO_4$ crystal $\varnothing 35 \times 40$ mm; (2) $ZnMoO_4$ crystal $\varnothing 20 \times 40$ mm; (3) Ge slab (photodetector); (4) NTD thermistors; (5) PTFE supporting elements; (6) Copper support of the detector covered by light reflector foil.

Table 4. Performance of 55 g and 160 g $ZnMoO_4$ detectors. QF denote quenching factor of α particle signals with respect to β particle signals for the same deposited energy (~ 5.4 MeV).

Parameter	55 g	160 g
Sensitivity of the heat channel (uV/MeV)	121	212
Light yield (keV/MeV)	0.98	0.96
QF	0.153	0.156

3.5 Low temperature tests

The operation of the scintillating bolometers with the produced $ZnMoO_4$ crystals at low temperatures was performed in the cryogenic laboratories of the CSNSM (Orsay). Two $ZnMoO_4$ samples (55 g and 160 g) were installed in a high-power dilution refrigerator with a large experimental space. A single photodetector, consisting of a 2" Ge disk and instrumented with a Neutron Transmutation Doped (NTD) Ge thermistor as a temperature sensor, identical to those attached to the $ZnMoO_4$ crystals, collected the scintillation light emitted by both samples (see figure 6).

The copper heat-sink temperature was stabilized at 18 mK, and the detector operation temperature was about 1 mK higher due to sensor biasing. Both samples and light detector performed well, with an excellent signal-to-noise ratio. Unfortunately, aboveground operation is marginally compatible with such large crystals. In the large detector, practically every time window containing a full pulse contains also other pulses.

It is possible to appreciate the pile-up effect in the inset of figure 7 where 4 seconds streaming data accumulated with a weak ^{232}Th gamma source are shown. It should be stressed that the pile-up remains substantial also for the background data acquired without calibration source. This affects the energy resolution of the detector, which is expected to be much better in underground operation under heavy shielding with much lower pile-up effect.

In spite of that, a preliminary useful characterization can be performed in terms of signal amplitude, light yield, light quenching factors for alpha particles and crystal radiopurity. The results for the two crystals are summarized in table 4. The difference in thermal response is due

2014 JINST 9 P06004

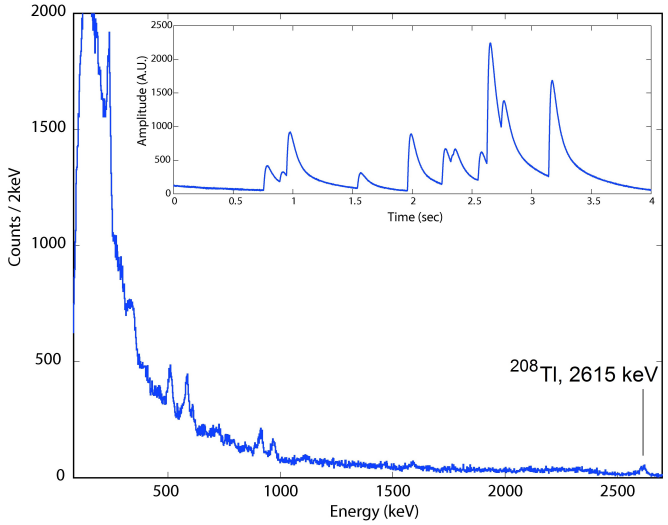

Figure 7. Energy spectrum accumulated by 160 g $ZnMoO_4$ bolometer with ^{232}Th γ source. (Inset) Typical pile-up effect due to the slow time response of the bolometric detector.

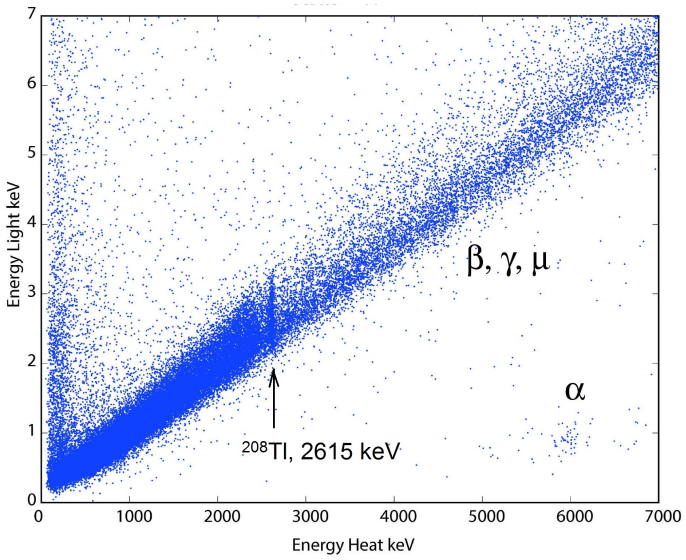

Figure 8. The scatter plot of light and heat signals for 160 g $ZnMoO_4$ crystal accumulated over 81 h in aboveground set-up in Orsay. The α band (populated mainly by ^{210}Po internal contamination of the crystal) is neatly separated from the β band (containing also γ quanta and cosmic muons). The energy scale is determined by a γ calibration (the 2615 keV γ line of ^{208}Tl is clearly appreciable). The cluster of α counts is due to an internal contamination of ^{210}Po, appearing at the fake energy of ~ 6 MeV (instead of ~ 5.4 MeV) due to a different thermal response of α particles with respect to γ and β radiation.

to the intrinsic irreproducibility of the thermal coupling in this type of detectors. The values of the quenching factor and of the light yield are perfectly compatible with those reported in the literature. Figure 7 shows a ^{232}Th calibration and figure 8 presents a light-heat scatter plot accumulated with the large 160 g $ZnMoO_4$ crystal. With the exception of the ^{210}Po line at 5.41 MeV, no internal alpha line emerged in the energy spectrum after about two weeks of data taking.

2014 JINST 9 P06004

4 Conclusions

The LUMINEU program aims at performing a pilot experiment on neutrinoless double beta decay of ^{100}Mo using radiopure $ZnMoO_4$ crystals operated as scintillating bolometers. This requires the development of methods of molybdenum purification to obtain crystals with the desired characteristics.

Different approaches of molybdenum purification for $ZnMoO_4$ crystals growth were elaborated. A purification using two-stage sublimation (with addition of zinc molybdate) and recrystallization from aqueous solutions of ammonium para-molybdate (using zinc molybdate as a collector) is a promising approach to purify molybdenum for high quality radiopure $ZnMoO_4$ crystals growth.

A first batch of LUMINEU crystals with mass of the crystal boules up to 1.5 kg have been successfully grown by the low-thermal-gradient Czochralski technique, and their optical, luminescent, diamagnetic, thermal and bolometric properties were tested. Further characterization of the material is in progress, in particular as far as its radiopurity level is concerned.

Further studies of radioactive contamination, luminescence, optical and bolometric properties will be performed to set a number of necessary purification steps. An as low as possible radioactive contamination would be surely a benefit to perform a large scale double beta decay experiment capable to explore the inverted neutrino mass hierarchy. Therefore, an as deep as possible purification of the initial materials for $ZnMoO_4$ crystal production looks a crucial task. In the future, crystals of increasing mass from deep purified precursors will be developed for the LUMINEU experiment, including crystals enriched in the isotope ^{100}Mo.

Acknowledgments

The development of $ZnMoO_4$ scintillating bolometers is part of the LUMINEU program, a project receiving funds from the Agence Nationale de la Recherche (France). The work was supported in part by the project "Cryogenic detector to search for neutrinoless double beta decay of molybdenum" in the framework of the Programme "Dnipro" based on Ukraine-France Agreement on Cultural, Scientific and Technological Cooperation. The bolometric tests were assisted by ISOTTA, a project receiving funds from the ASPERA 2nd Common Call dedicated to R&D activities. The group from the Institute for Nuclear Research (Kyiv, Ukraine) was supported in part by the Space Research Program of the National Academy of Sciences of Ukraine.

References

[1] W. Rodejohann, *Neutrino-less Double Beta Decay and Particle Physics*, *Int. J. Mod. Phys.* **E 20** (2011) 1833 [arXiv:1106.1334].

[2] S.R. Elliott, *Recent Progress in Double Beta Decay*, *Mod. Phys. Lett.* **A 27** (2012) 1230009 [arXiv:1203.1070].

[3] J.D. Vergados, H. Ejiri and F. Simkovic, *Theory of Neutrinoless Double Beta Decay*, *Rept. Prog. Phys.* **75** (2012) 106301 [arXiv:1205.0649].

[4] A. Giuliani and A. Poves, *Neutrinoless Double-Beta Decay*, *Adv. High En. Phys.* **2012** (2012) 857016.

2014 JINST 9 P06004

[5] R.N. Mohapatra et al., *Theory of neutrinos: a white paper*, *Rept. Prog. Phys.* **70** (2007) 1757 [hep-ph/0510213].

[6] G.L. Fogli et al., *Observables sensitive to absolute neutrino masses: a reappraisal after WMAP-3y and first MINOS results*, *Phys. Rev.* **D 75** (2007) 053001 [hep-ph/0608060].

[7] G.L. Fogli et al., *Observables sensitive to absolute neutrino masses. II.*, *Phys. Rev.* **D 78** (2008) 033010 [arXiv:0805.2517].

[8] A.S. Barabash, *Precise half-life values for two neutrino double beta decay*, *Phys. Rev.* **C 81** (2010) 035501 [arXiv:1003.1005].

[9] R. Saakyan, *Two-Neutrino Double-Beta Decay*, *Ann. Rev. Nucl. Part. Sci.* **63** (2013) 503.

[10] O. Cremonesi and M. Pavan, *Challenges in Double Beta Decay*, *Adv. High En. Phys.* **2104** (2014) 951432 [arXiv:1310.4692].

[11] S. Rahaman et al., *Q value of the ^{76}Ge and ^{100}Mo Double-Beta Decay*, *Phys. Lett.* **B 662** (2008) 111 [arXiv:0712.3337].

[12] M.E. Wieser and J.R.D. Laeter, *Absolute isotopic composition of molybdenum and the solar abundances of the p-process nuclides ^{92,94}Mo*, *Phys. Rev.* **C 75** (2007) 055802.

[13] NEMO-3 collaboration, L. Simard, *The NEMO-3 results after completion of data taking*, *J. Phys. Conf. Ser.* **375** (2012) 042011.

[14] S. Pirro et al., *Scintillating double beta decay bolometers*, *Phys. Atom. Nucl.* **69** (2006) 2109 [nucl-ex/0510074].

[15] A. Giuliani, *Neutrino Physics with Low-Temperature Detectors*, *J. Low Temp. Phys.* **167** (2012) 991.

[16] C. Arnaboldi et al., *$CdWO_4$ scintillating bolometer for Double Beta Decay: Light and Heat anticorrelation, light yield and quenching factors*, *Astropart. Phys.* **34** (2010) 143 [arXiv:1005.1239].

[17] S.J. Lee et al., *The development of a cryogenic detector with $CaMoO_4$ crystals for neutrinoless double beta decay search*, *Astropart. Phys.* **34** (2011) 732.

[18] J.W. Beeman et al., *A next generation neutrinoless double beta decay experiment based on $ZnMoO_4$ scintillating bolometers*, *Phys. Lett.* **B 710** (2012) 318 [arXiv:1112.3672].

[19] J.W. Beeman et al., *$ZnMoO_4$: A promising bolometer for neutrinoless double beta decay searches*, *Astropart. Phys.* **35** (2012) 813 [arXiv:1202.0238].

[20] J.W. Beeman et al., *Performances of a large mass ZnSe bolometer to search for rare events*, 2013 *JINST* **8** P05021 [arXiv:1303.4080].

[21] L. Gironi et al., *Performance of $ZnMoO_4$ crystal as cryogenic scintillating bolometer to search for double beta decay of molybdenum*, 2010 *JINST* **5** P11007 [arXiv:1010.0103].

[22] J.W. Beeman et al., *An improved $ZnMoO_4$ scintillating bolometer for the search for neutrinoless double beta decay of ^{100}Mo*, *J. Low Temp. Phys.* **167** (2012) 1021.

[23] J.W. Beeman et al., *Performances of a large mass $ZnMoO_4$ scintillating bolometer for a next generation 0νDBD experiment*, *Eur. Phys. J.* **C 72** (2012) 2142.

[24] D.M. Chernyak et al., *Optical, luminescence and thermal properties of radiopure $ZnMoO_4$ crystals used in scintillating bolometers for double beta decay search*, *Nucl. Instrum. Meth.* **A 729** (2013) 856.

[25] L.I. Ivleva et al., *Growth and Properties of $ZnMoO_4$ Single Crystals*, *Crystallogr. Rep.* **53** (2008) 1087 [*Kristallografiya* **53** (2008) 1145].

2014 JINST 9 P06004

[26] W. Reichelt et al., *Mischkristallbildung im System $CuMoO_4/ZnMoO_4$*, Z. Anorg. Allg. Chem. **626** (2000) 2020.

[27] L.L. Nagornaya et al., *Tungstate and molybdate scintillators to search for dark matter and double beta decay*, IEEE Trans. Nucl. Sci. **56** (2009) 2513.

[28] D. Spassky et al., *Luminescence investigation of zinc molybdate single crystals*, Phys. Status Solidi **A 206** (2009) 1579.

[29] M Laubenstein et al., *Underground measurements of radioactivity*, Appl. Radiat. Isot. **61** (2004) 167.

[30] P. Belli et al., *New observation of $2\beta 2\nu$ decay of ^{100}Mo to the 0_1^+ level of ^{100}Ru in the ARMONIA experiment*, Nucl. Phys. **A 846** (2010) 143.

[31] A.N. Zelikman and B.G. Korshunov, *Metallurgy of Rare Metals* (in Russian), Metallurgy, Moscow, Russia (1991).

[32] A.A. Pavlyuk et al., *Low Thermal Gradient technique and method for large oxide crystals growth from melt and flux*, in Proceedings of *The APSAM-92, Asia Pacific Society for Advanced Materials*, Shanghai, P.R.C., 26–29 April 1992, Institute of Materials Research, Tohoku University, Sendai, Japan, 1993, pg. 164.

[33] Yu.A. Borovlev et al., *Progress in growth of large sized BGO crystals by the low-thermal-gradient Czochralski technique*, J. Cryst. Growth **229** (2001) 305.

[34] E.N. Galashov et al., *Growing of $^{106}CdWO_4$, $ZnWO_4$ and $ZnMoO_4$ scintillation crystals for rare events search by low thermal gradient Czochralski technique*, *Funct. Mater.* **17** (2010) 504.

[35] A.M. Dubovik et al., *Research and development of $ZnBO_4$ $(B = W, Mo)$ crystal scintillators for dark matter and double beta decay searching*, *Acta Phys. Pol.* **A 117** (2010) 15.

[36] L.L. Nagornaya et al., *Research and development of alkali earth tungstate and molybdate crystal scintillators for search for rare events*, *Funct. Mater.* **16** (2009) 54.

[37] L.G. Van Uitert et al., *Preparation of Single Crystal of Tungstates and Molybdates of a Number of Divalent Metal Ions*, J. Am. Ceram. Soc. **46** (1963) 512.

[38] J.E. Gordon et al., *Specific heat data of high-T_c superconductors: Lattice and electronic contributions*, Solid State Comm. **69** (1989) 625.

2014 JINST 9 P06004